Biophysical Journal

Supporting Material

Probing the Structural and Dynamical Effects of the Charged Residues of the TZF Domain of TIS11d

Brittany R. Morgan,[1] Laura M. Deveau,[1] and Francesca Massi[1,*]

[1]Department of Biochemistry and Molecular Pharmacology, University of Massachusetts, Worcester, Massachusetts

Supplemental Table and Figures

Temperature (° C)	TIS11d $K_{d,app}$ (nM)	TIS11d-Δ D219/E220 $K_{d,app}$ (nM)
26	7.8 ± 1.4	17 ± 3
29	12 ± 2	29 ± 3
32	16 ± 4	49 ± 10
35	30 ± 8	78 ± 4
38	58 ± 12	151 ± 36

Table S1. Mean and error of $K_{d,app}$ by temperature for TIS11d and TIS11d-Δ D219/E220.

	ZF1 RMSD (Å)	ZF2 RMSD (Å)
TIS11d	2.20 ± 0.04	2.07 ± 0.07
TIS11d-E220A	2.20 ± 0.12	2.13 ± 0.06
TIS11d-Δ D219/E220	2.27 ± 0.10	2.34 ± 0.31

Table S2. Mean and standard deviation of RMSD from NMR structure of ZF1 and ZF2. RMSD was calculated after alignment on each finger domain, respectively, and averaged over the three trajectories for each system.

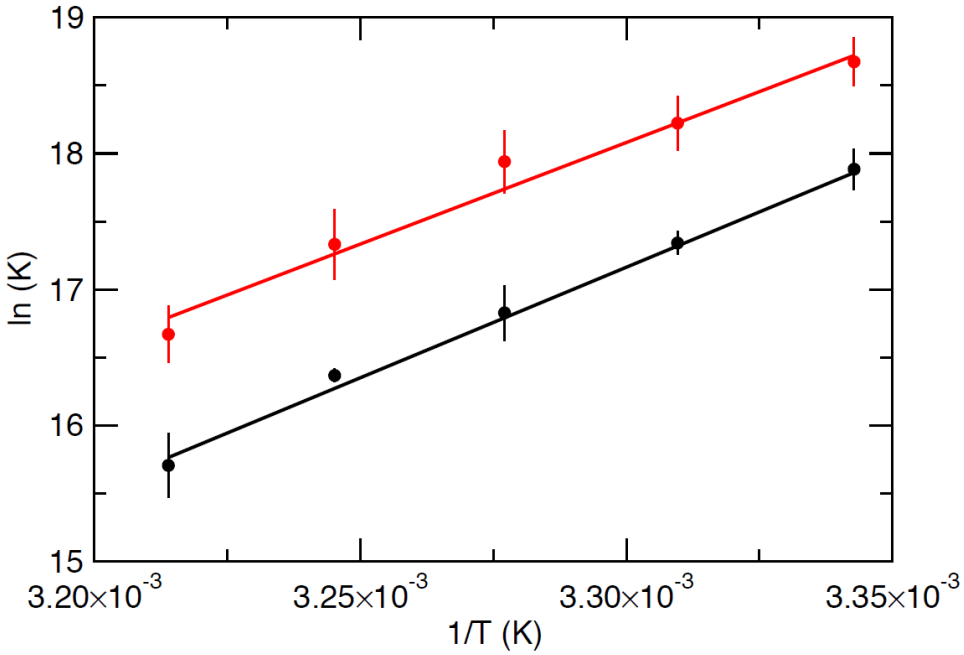

Figure S1. Van't Hoff plots for TIS11d and TIS11d-Δ D219/E220. The equilibrium dissociation constants ($K_{d,app}$), calculated from fitting the fluorescence polarization data at each temperature, are shown as a function of the temperature for TIS11d (red circles) and TIS11d-Δ D219/E220 (black circles). The straight lines show the linear plots of the van't Hoff equation obtained using ΔH and ΔS determined from the global fit (Table 1) of the binding data for TIS11d (red) and TIS11d-Δ D219/E220 (black).

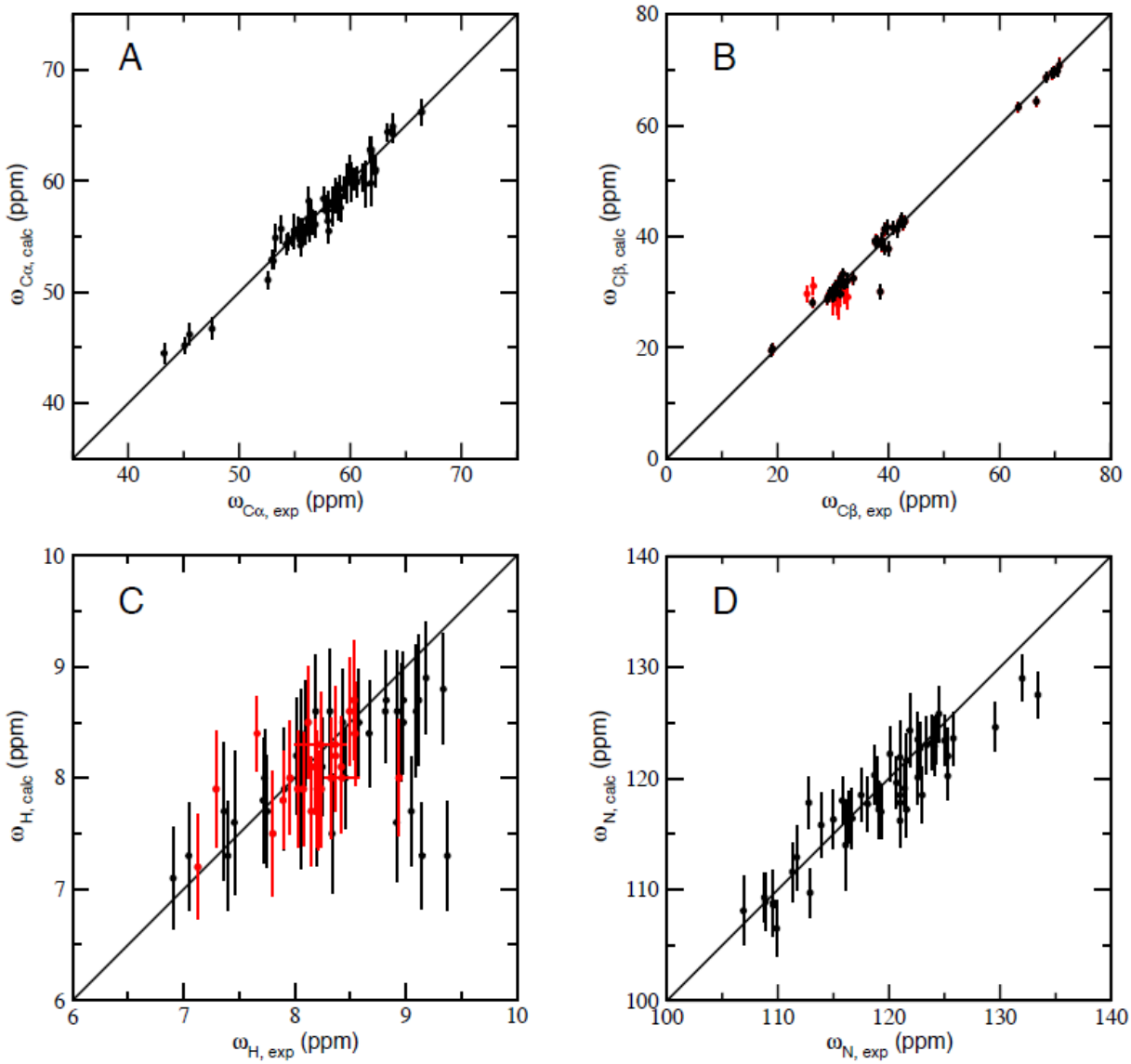

Figure S2. Correlation of chemical shifts for TIS11d (shifts predicted from MD trajectories versus NMR experimental data) for A: Cα, B: Cβ, C: H^N and D: N^H. In (B) the CCCH residues that coordinate the Zn^{2+} ions are shown in red (empirical chemical shift programs do not account for metal ions). In (C), residues more than 8 Å away from the Zn^{2+} ions are highlighted in red. The correlation coefficients were 0.98 for Cα, 0.99 for Cβ, 0.56 for H, and 0.92 for N.

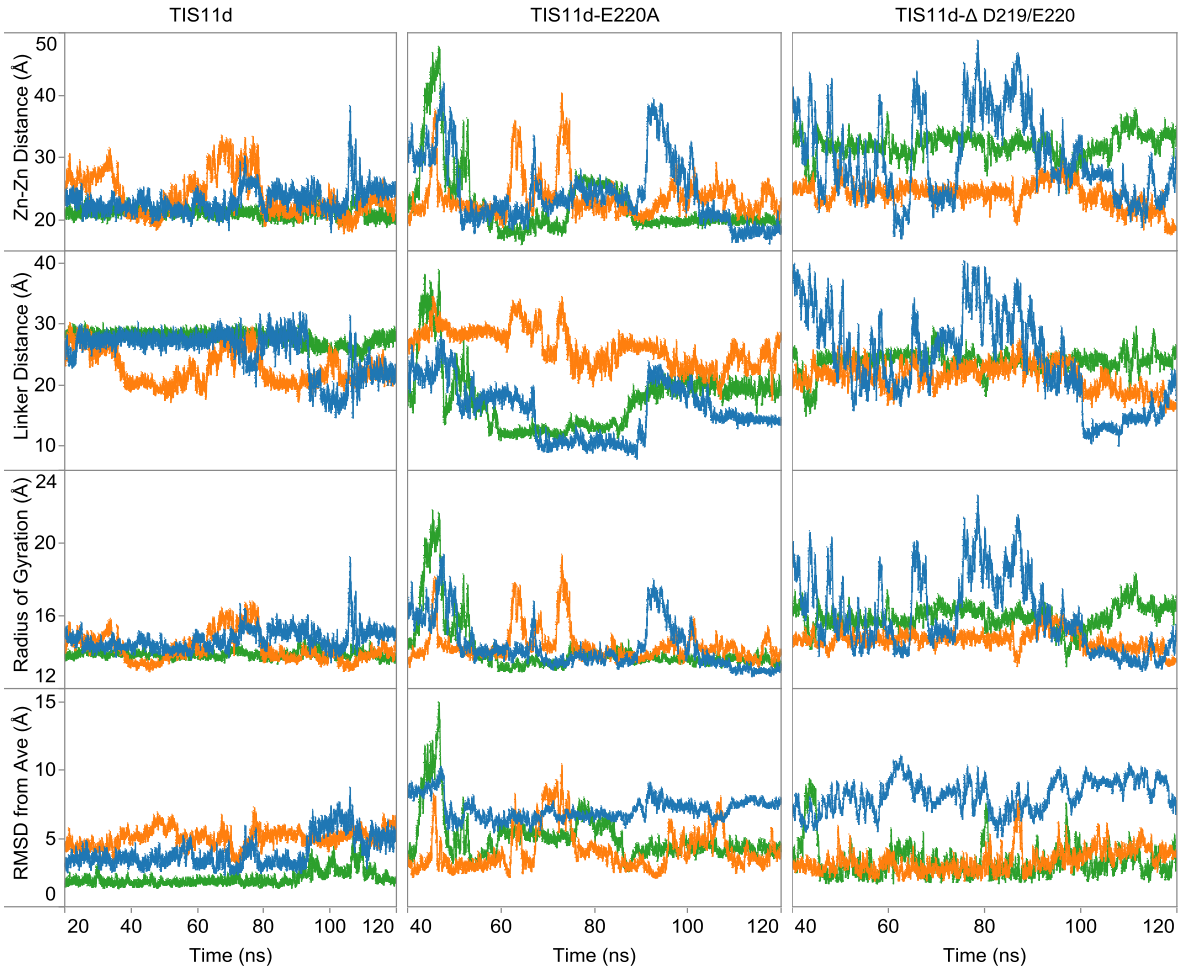

Figure S3. Dynamic behavior of structural metrics for each system (as labeled) as a function of time by trajectory (trajectories 1, 2, and 3 are blue, orange, and green, respectively).

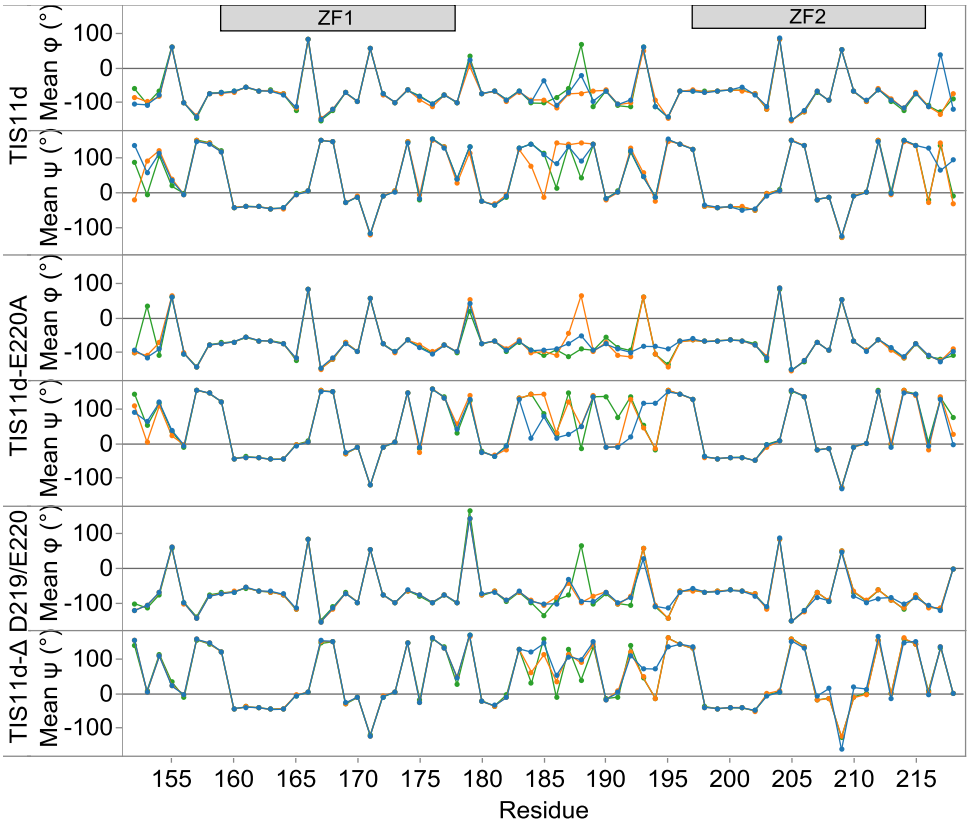

Figure S4. Mean backbone dihedral angles for each trajectory (trajectories 1, 2, and 3 are blue, orange, green, respectively) for each of the three systems (as labeled).

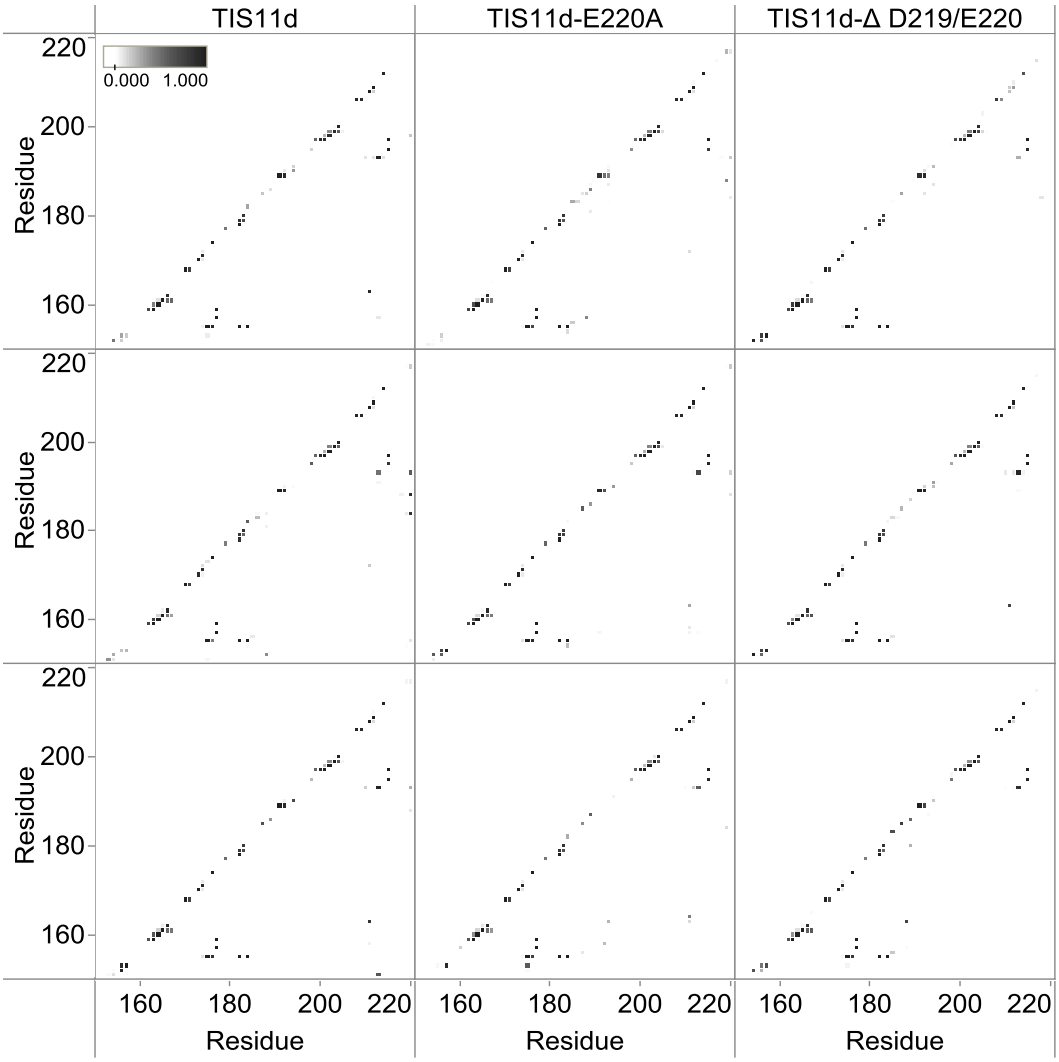

Figure S5. Hydrogen bond probability maps by trajectory (rows 1-3) for each system (columns 1-3, as labeled).

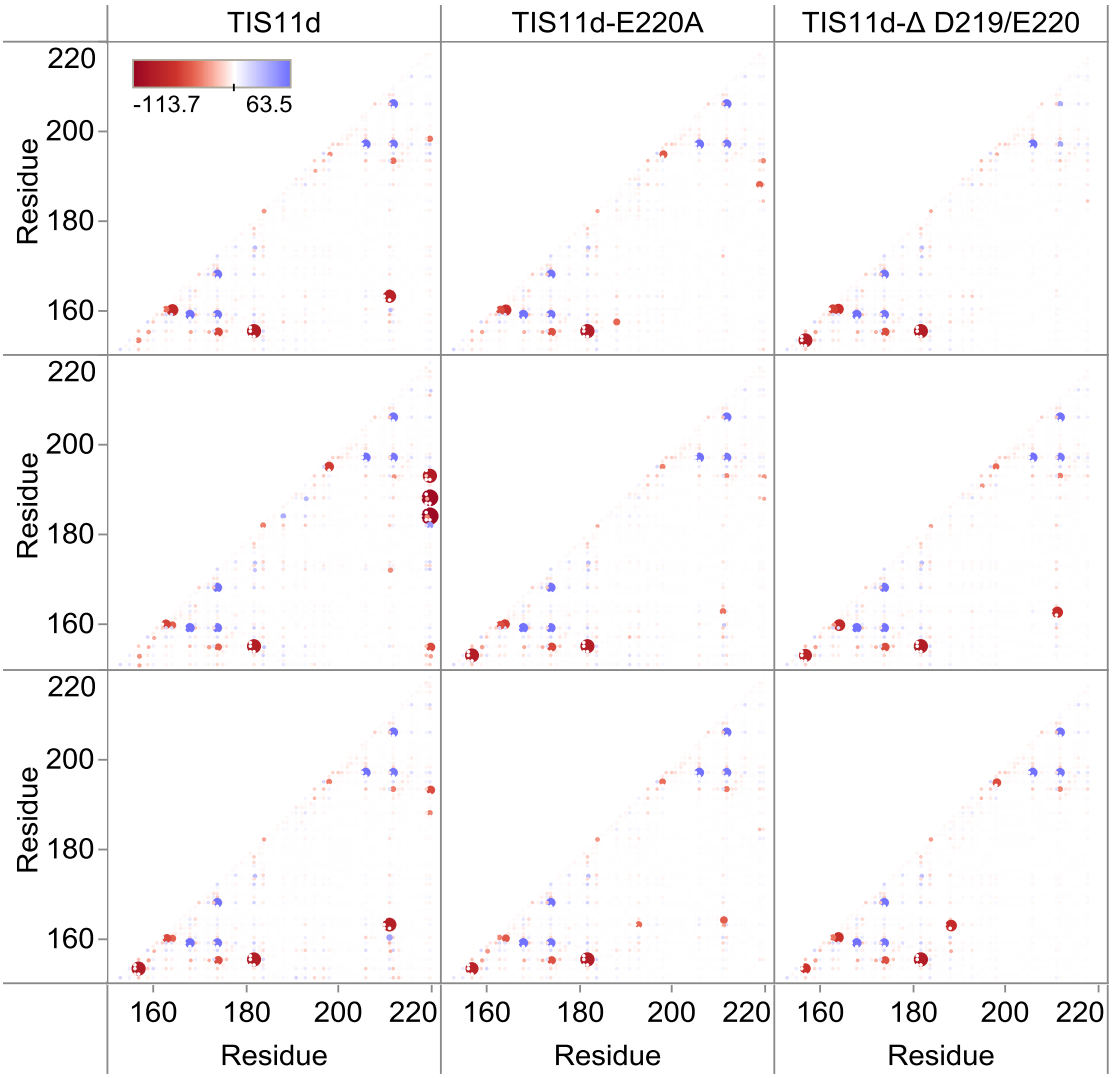

Figure S6. Interaction energy between residue pairs by trajectory (rows 1-3) for each of the three systems (columns 1-3, as labeled). Size of circles is a function of the interaction strength to highlight strong interactions, the larger the circle the stronger the interaction.

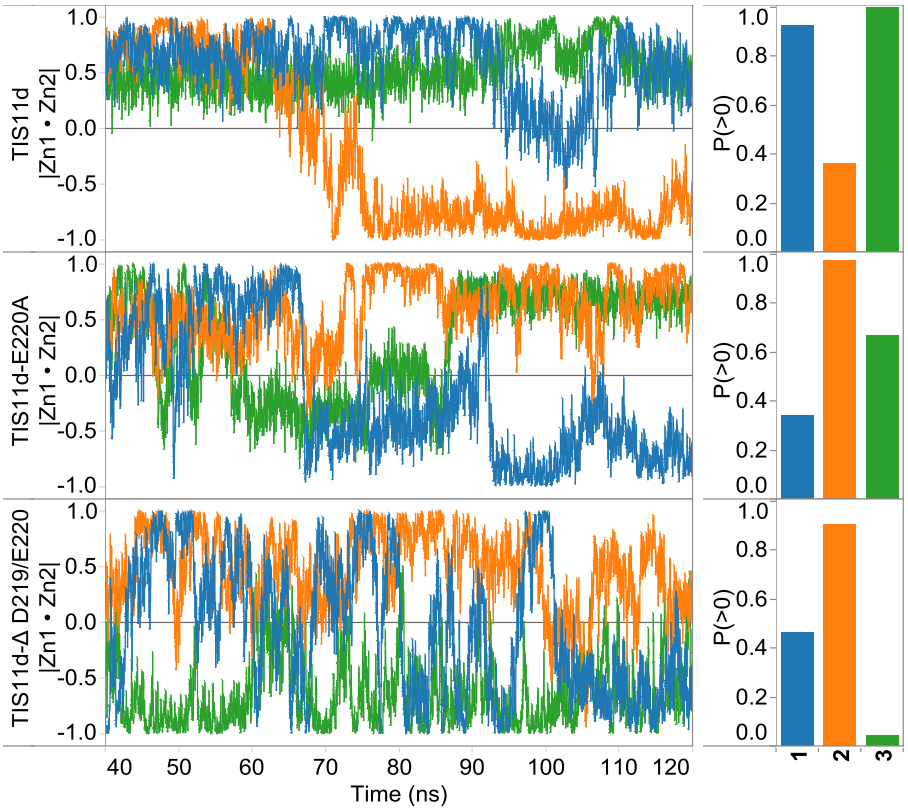

Figure S7. Characterization of zinc finger relative orientation for each system (as labeled). Left: The dot product of the two zinc finger vectors as a function of time, colored by trajectory (blue, orange, green). Right: The proportion of the trajectory where the dot product is greater than zero.

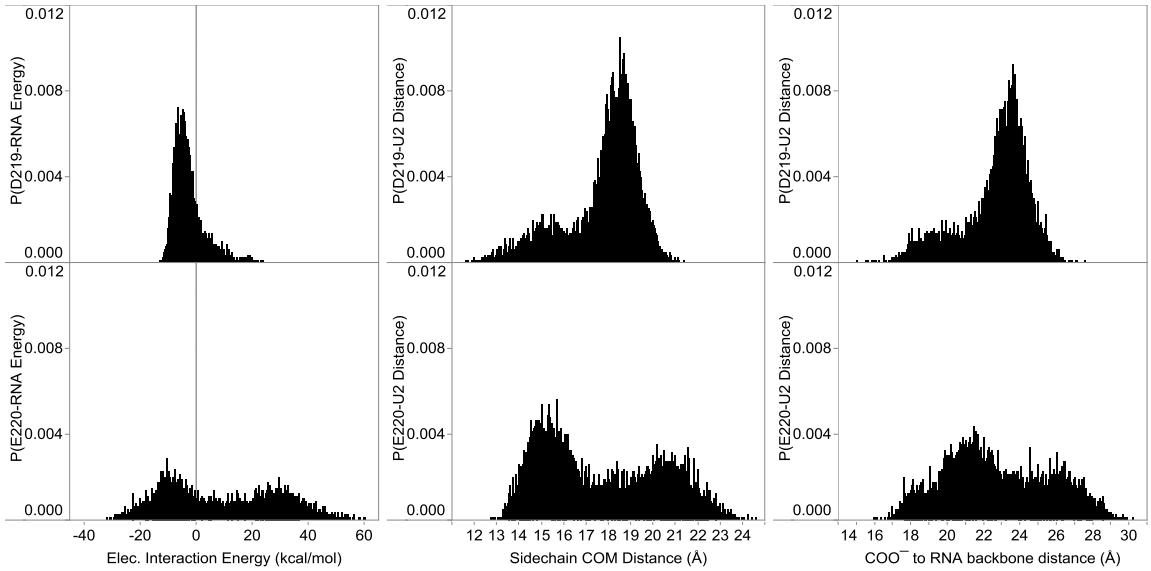

Figure S8. Interaction between negative C-terminus residues of TIS11d and RNA (combined trajectories). Left: Electrostatic interaction energy of D219 and E220 with RNA. Middle: center of mass (COM) distance between the side-chains of D219 and E220 and the base ring of U2, the closest RNA base. Right: the distance between the COO^- groups of D219 and E220 and the backbone of U2.